上海大学 Shanghai University | 力学与工程科学学院 School of Mechanics and Engineering Science | 上海市应用数学和力学研究所 Shanghai Institute of Applied Mathematics and Mechanics

# Microstructure Evolution in Sintering of Refractory Materials: Phase-Field-Micromechanics Modeling

**Qingcheng Yang (杨庆成)[1], Arkadz Kirshtein[2], Pin Wu[3], Qiang Zhen[4,5]**

[1]School of Mechanics and Engineering Science, Shanghai Institute of Applied Mathematics and Mechanics, Shanghai University, Shanghai, 200072, China
[2]Department of Mathematics & Statistics, Texas A&M University-Corpus Christi, Corpus Christi, TX 78412, USA
[3]School of Computer Engineering and Science, Shanghai University, Shanghai 200444, China
[4]Nano-Science and Technology Research Center, Shanghai University 200072, China
[5]School of Materials Science and Engineering, Shanghai University 200072, China

**The 9TH International Symposium on Refractories**
**Oct. 15-18, 2024， Chengdu, China**

# Solid State Sintering of Crystalline Materials

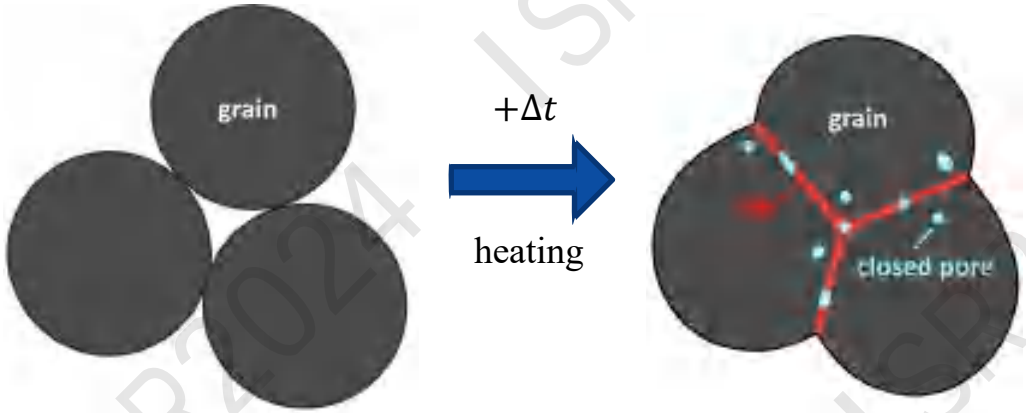


Solid state sintering is the thermal consolidation of discrete powder ensembles to build a coherent compact component at elevated temperature (but below the melting point).

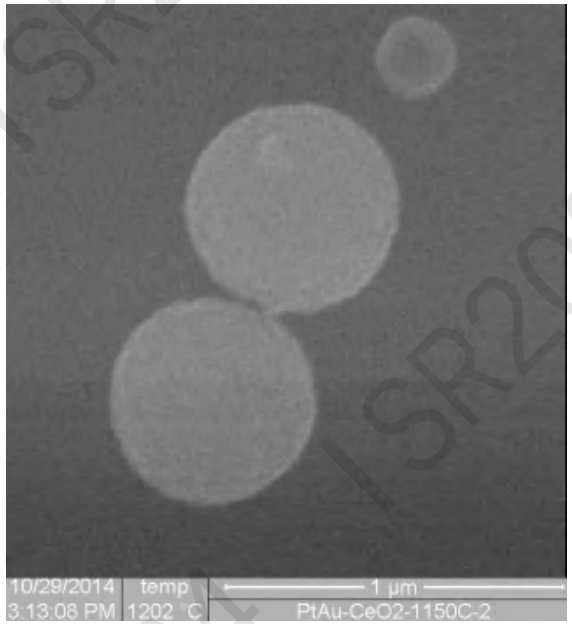


Experimental observations of polycrystalline microspheres sintering at T = 1150 ℃ using environmental scanning electron microscope at high temperature (HT-ESEM).

A. Nommeots-Nomm et al, Mater. Today Adv., 2019

# Viscous Sintering of Polymer

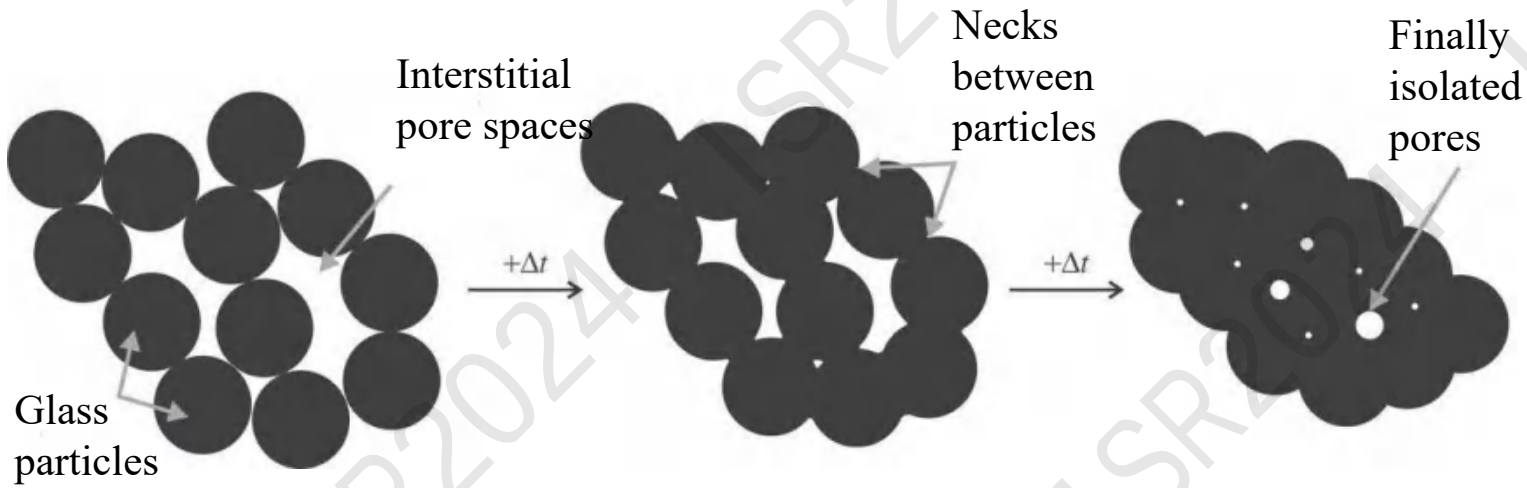


Viscous sintering is a process in which thermal energy is utilized to densify and strengthen a powder compact driven by surface energy reduction without forming any boundaries.

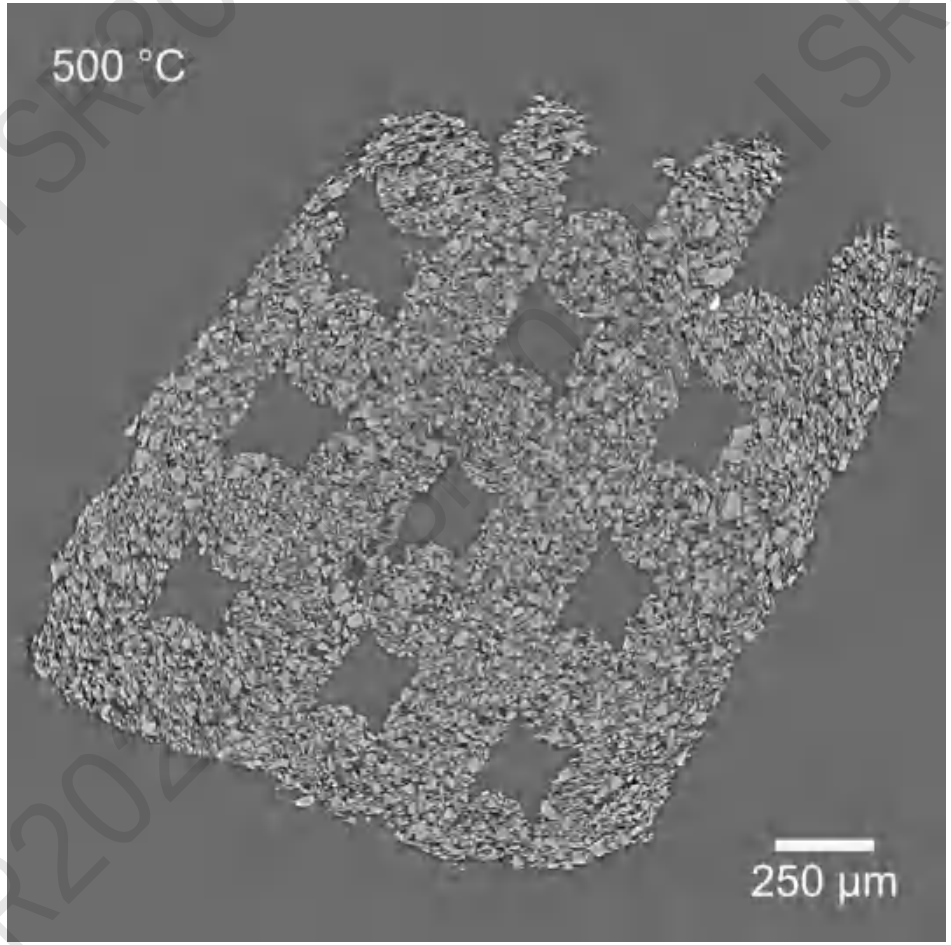


Viscous sintering of a 3D printed bioactive glass scaffold using synchrotron X-ray tomography.

A. Nommeots-Nomm et al, Mater. Today Adv., 2019

# Outlines

- Phase-Field-Micromechanics Modeling of Microstructure Evolution in Viscous Sintering: Polymers

- Phase-Field-Micromechanics Modeling of Microstructure Evolution in Solid-State Sintering : Ceramics and Metals

# Phase-Field-Micromechanics Modeling of Microstructure Evolution in Viscous Sintering

## Mass Transport Mechanisms

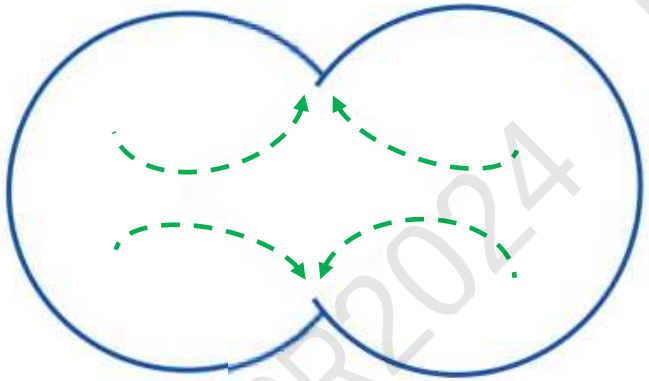

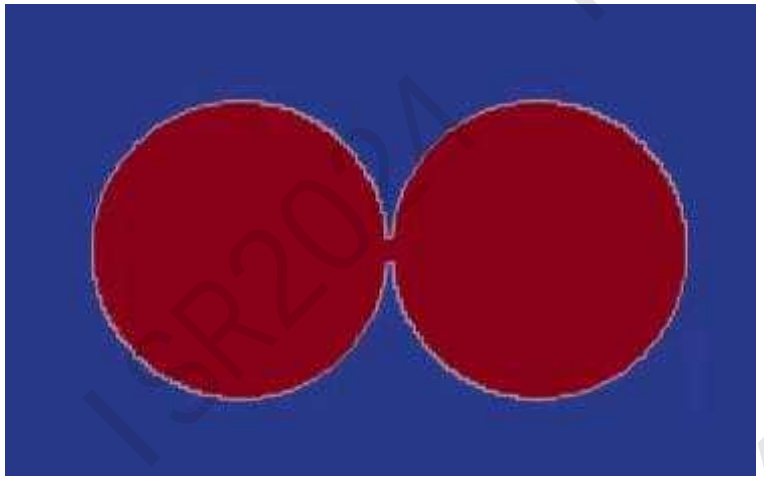

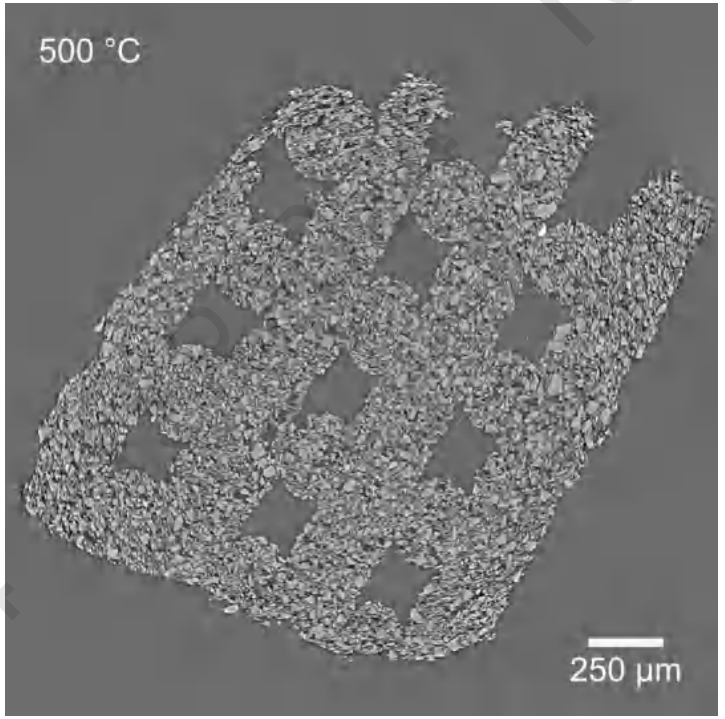


Viscous Flow

# Phase-Field-Micromechanics Modeling of Microstructure Evolution in Viscous Sintering

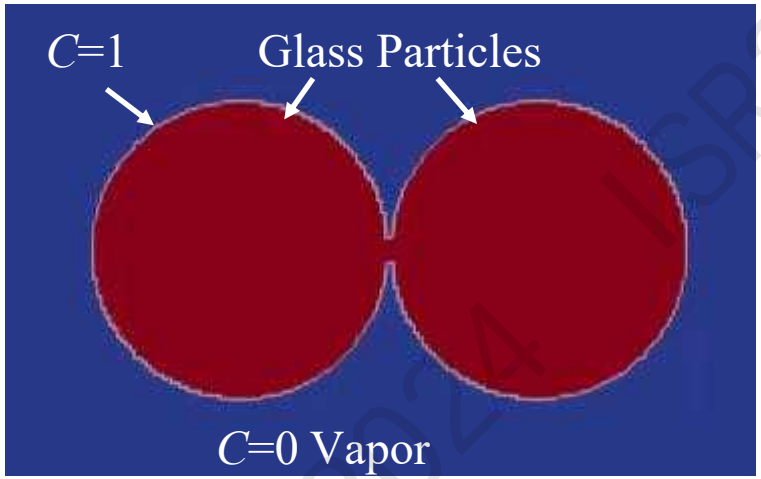


$$\Pi = \int_{\Omega} \left[ \rho \frac{\|\mathbf{v}\|^2}{2} + f(C) + \frac{\kappa_c}{2} \|\nabla C\|^2 \right] d\Omega$$

Kinetic Energy

Surface Energy

$$f(C) = AC^2(1-C)^2$$

$$A = \frac{3\gamma}{8\sqrt{2}\varepsilon}, \quad k_c = \frac{3\gamma\varepsilon}{2\sqrt{2}}$$

**Governing Equations:**

$\gamma$ : Specific energy

$\varepsilon$: Interfacial thickness

$$\frac{\partial C}{\partial t} = \nabla \cdot \left[ M \nabla \frac{\delta \Pi}{\delta C} \right] - \nabla \cdot (\mathbf{v}C)$$

$$\rho(C)\left[\frac{\partial \mathbf{v}}{\partial t} + \mathbf{v} \cdot \nabla \mathbf{v}\right] = -\nabla p + \nabla \cdot [\mu(C)(\nabla \mathbf{v} + (\nabla \mathbf{v})^T)] - \nabla \cdot \left(\frac{\partial \Pi}{\partial \nabla C} \otimes \nabla C\right)$$

Inertia force | Pressure | Viscous force | Surface tension

Incompressibility:

$$\nabla \cdot \mathbf{v} = 0$$

# Qualitative Experimental Validation

Microstructure evolution of ABS particle during sintering at 200 ℃

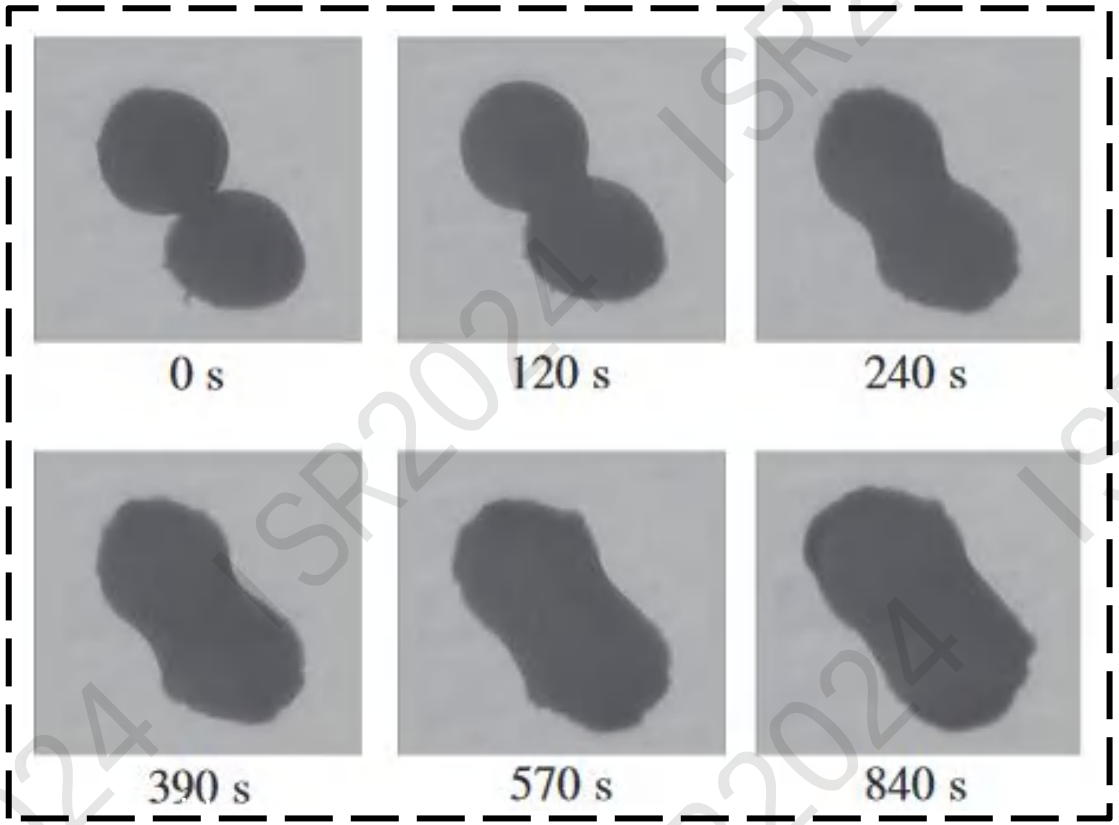


Experimental Observations

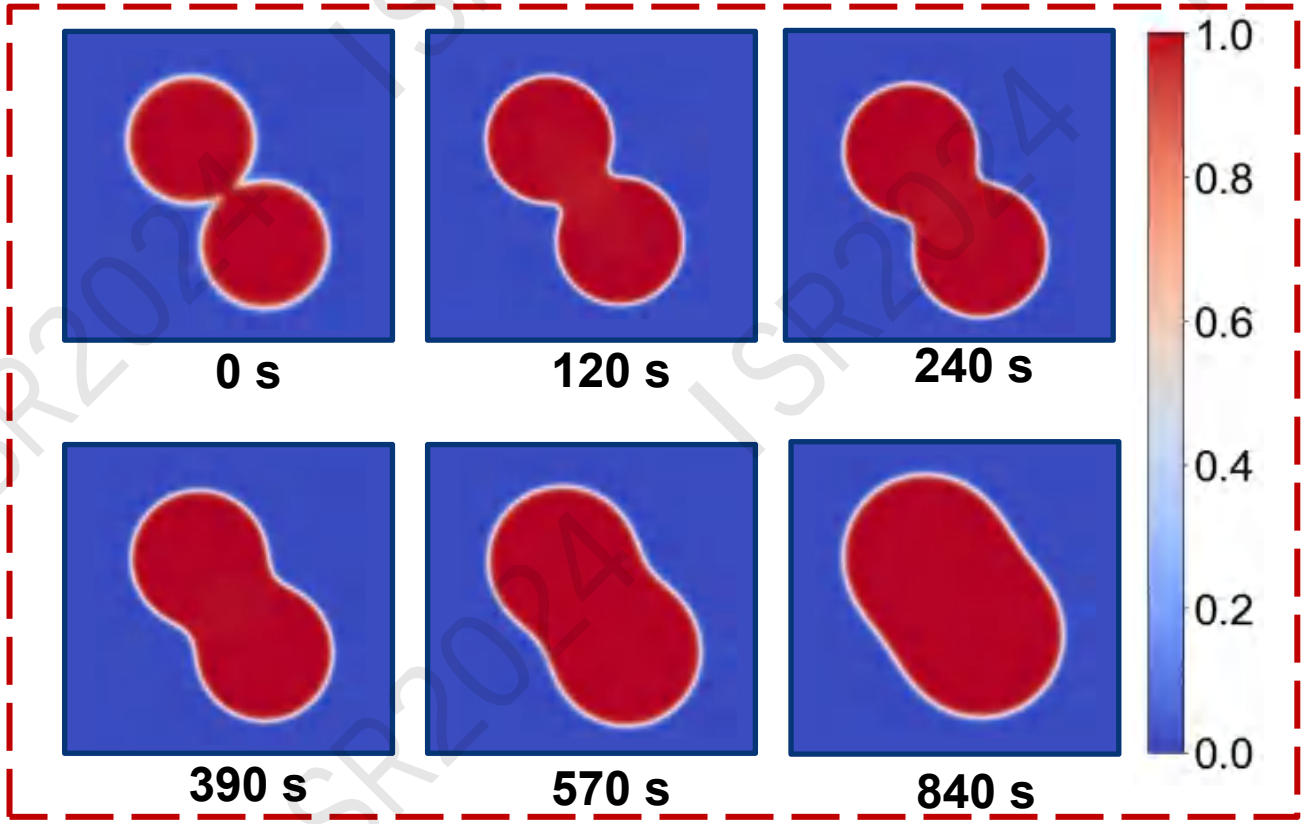


Phase-Field Simulation

# Quantitative Experimental Validation

Microstructure evolution of ABS particle during sintering at 240 ℃

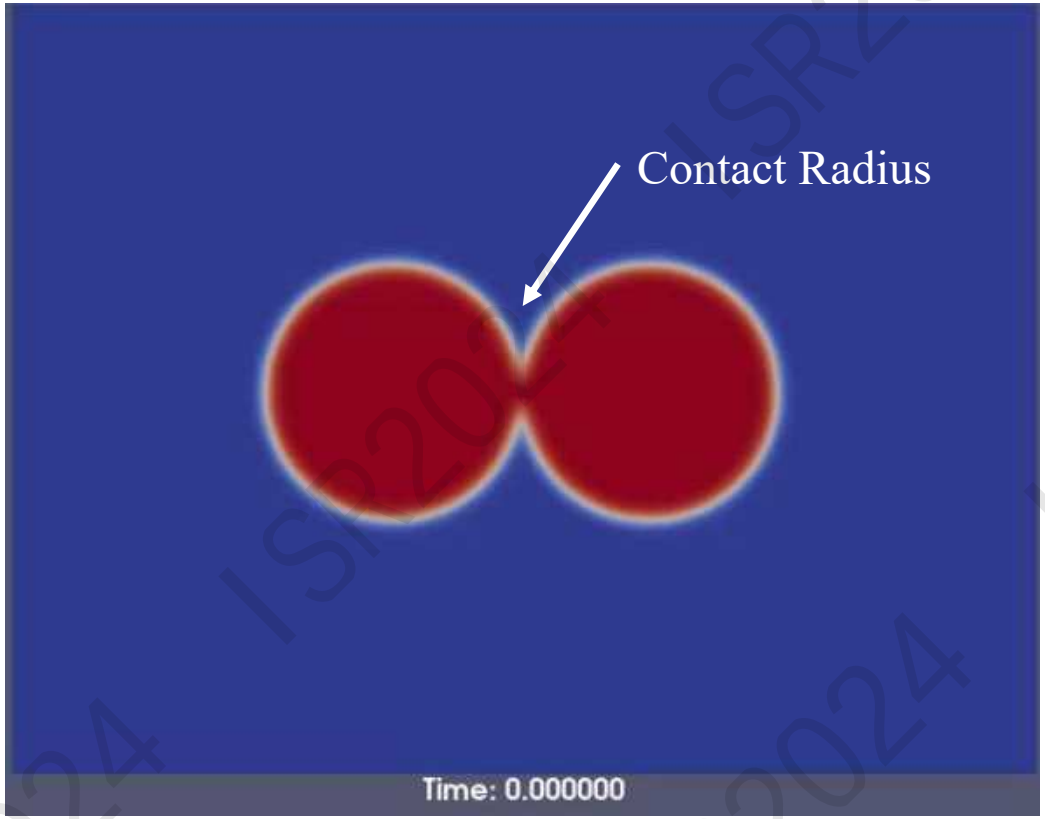


Phase-Field Simulation

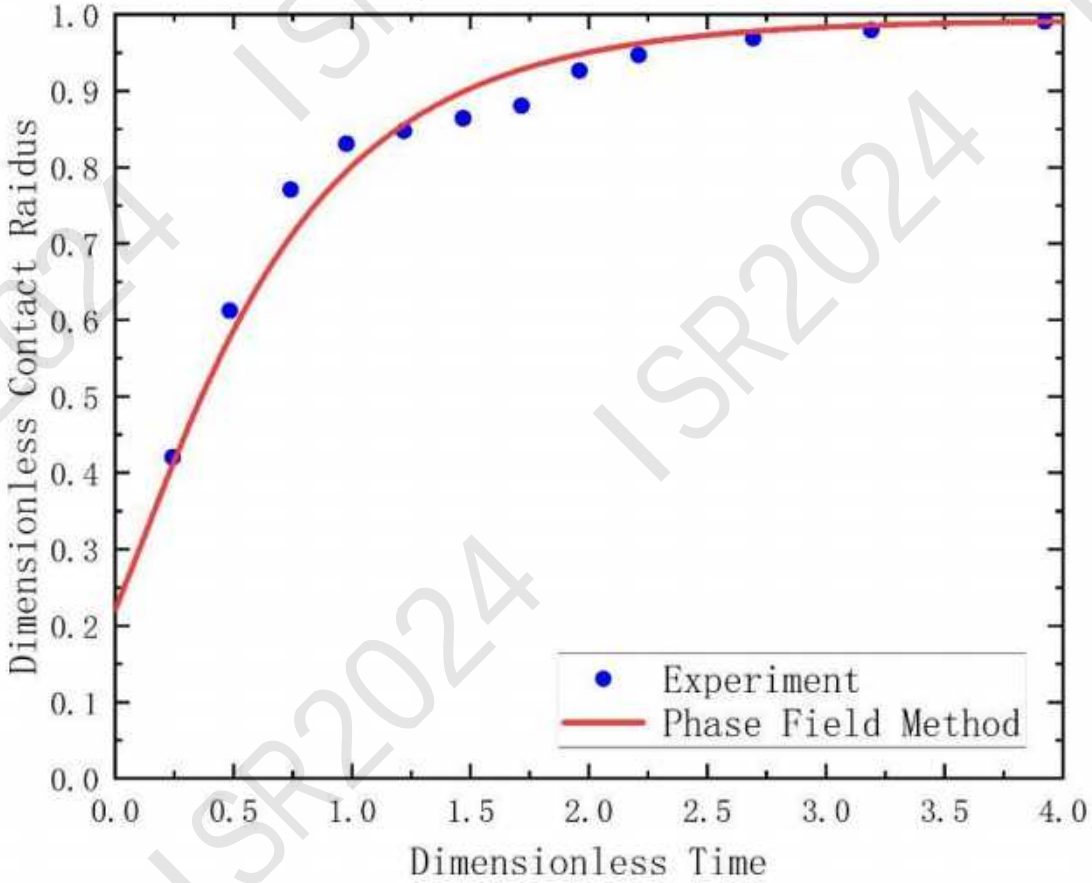


Comparison with experimental data

# Applications: Multi-particles

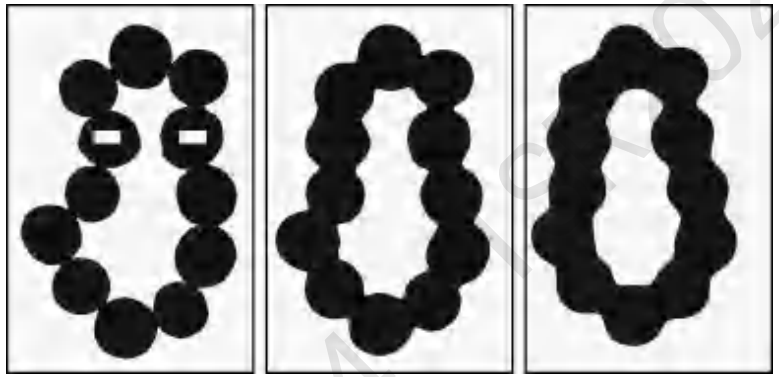

(a) Experimental observations

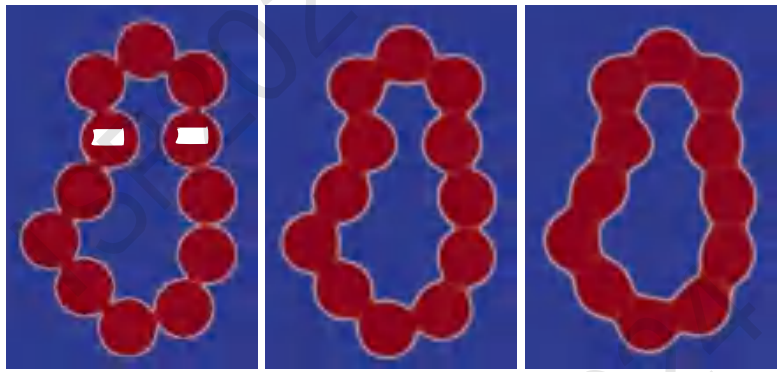

(b) Phase-Field simulation

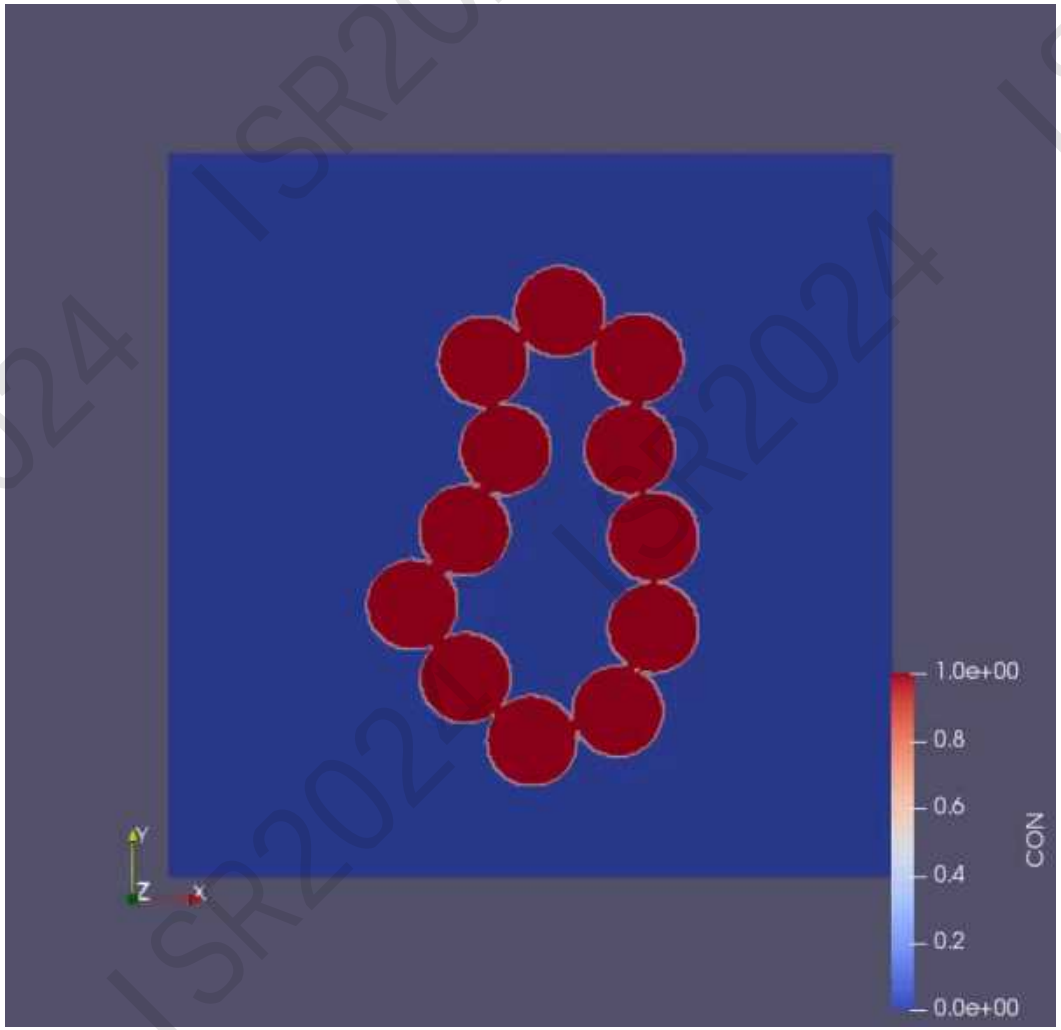


Particle rearrangement of the employed many-particle chain from experimental observations (a) (reproduced with permission from John Wiley and Sons) and phase-field simulations (b).

# Outlines

- Phase-Field-Micromechanics Modeling of Microstructure Evolution in Viscous Sintering: Polymers

- **Phase-Field-Micromechanics Modeling of Microstructure Evolution in Solid-State Sintering : Ceramics and Metals**

# Solid State Sintering Mechanisms

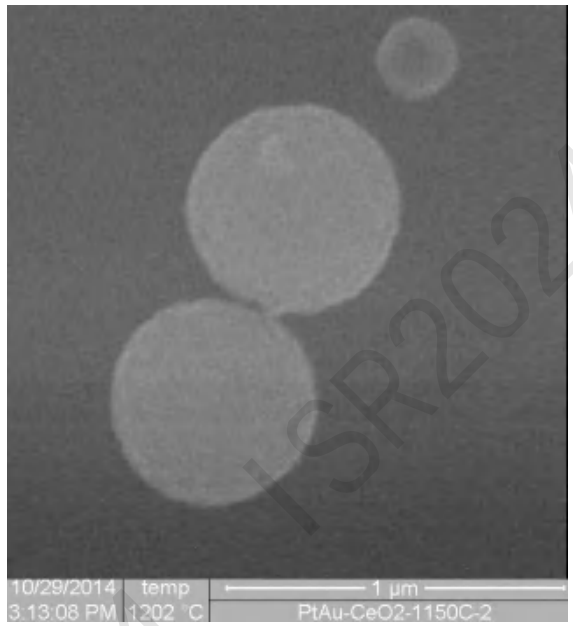


**Mass Transport Mechanisms**

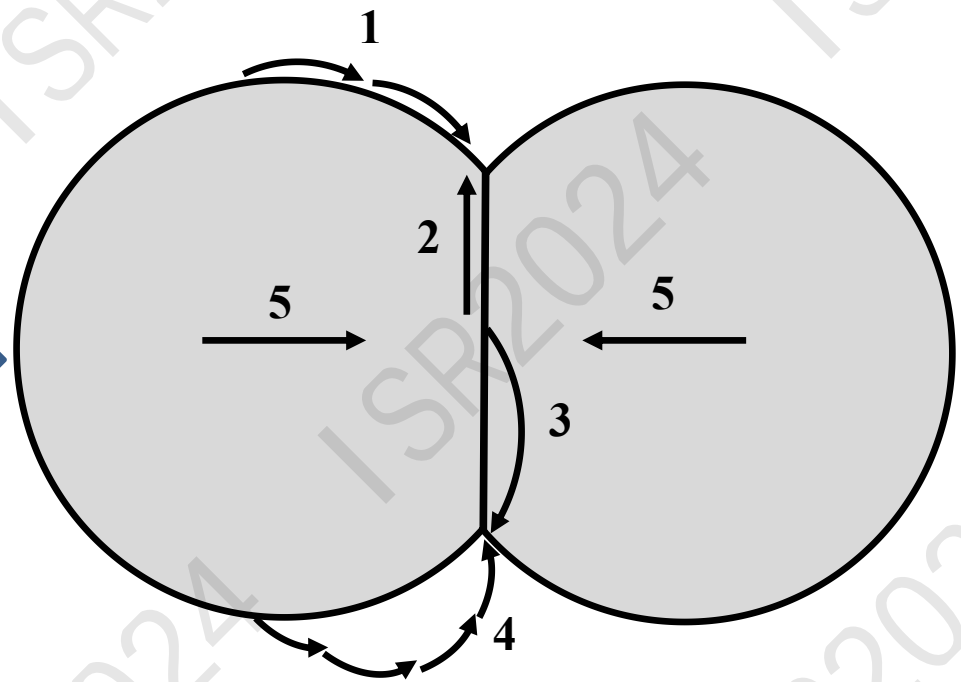


1. Surface Diffusion
2. Grain Boundary Diffusion
3. Volume Diffusion
4. Evaporation-Condensation
5. Grain Motion



R. German, Sintering: From Empirical Observations to Scientific Principles, 2014; F. Wakai, K.A Brakke, Acta Mater., 2011; F. Wakai, G. Okuma, Acta Mater., 2022

# Phase-Field-Micromechanics Modeling of Microstructure Evolution in Solid-State Sintering

1: Surface Diffusion
2: Grain Boundary Diffusion
3: Volume Diffusion
4: Evaporation-Condensation

$D_{surf}$: Surface Diffusivity
$D_{gb}$: Grain Boundary Diffusivity
$D_{vol}$: Volume Diffusivity
$D_{vap}$: Vapor Path Diffusivity
$D_{eff}$: Effective Diffusivity

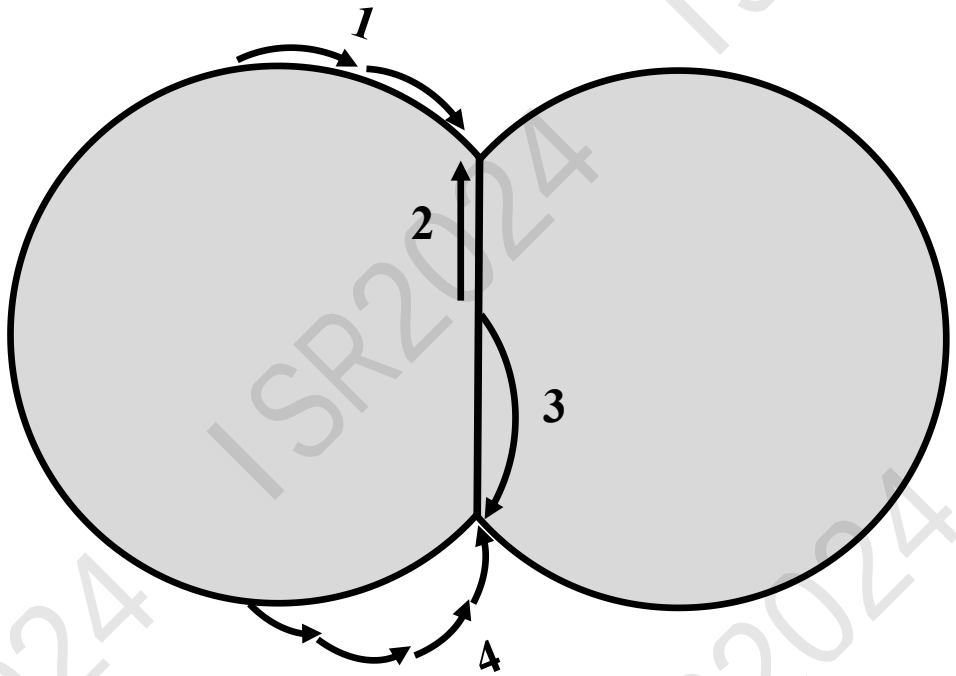


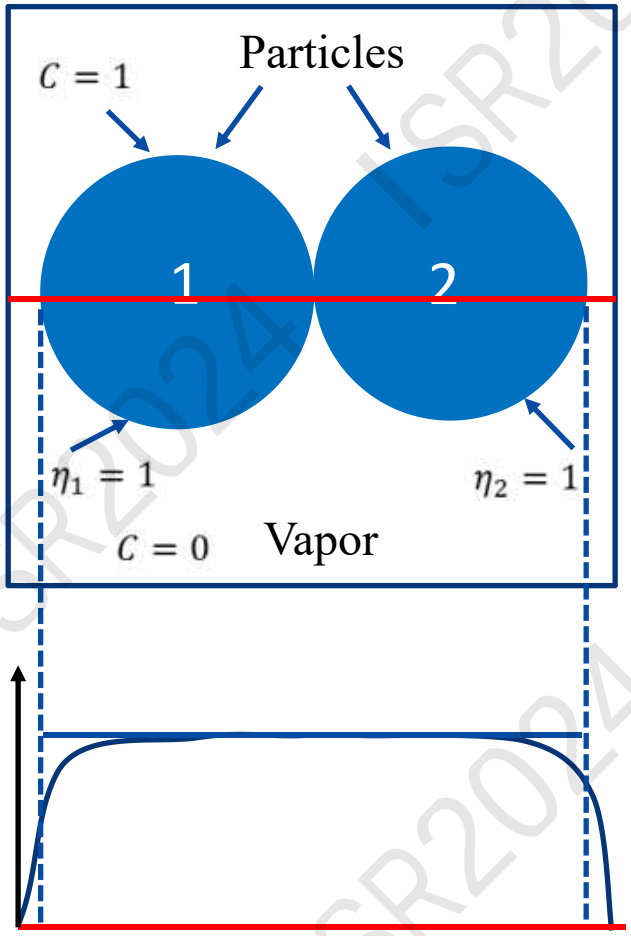


C: a phase-field to differentiate grain particles from surrounding medium

$\eta_i$: a phase-field to differentiate different grains

$$D_{eff} = D_{surf}16(1-C)^2C^2 + D_{gb}\sum_i\sum_{j\neq i}16\eta_i{}^2\eta_j{}^2 + D_{vol}N(C) + D_{vap}[1-N(C)]$$

Surface | Grain Boundary | Volume | Vapor

A. _Kazaryan, et al, *Scripta Materialia*,1999; Y.U. Wang, *Acta Mater.*, 2006; R. Shi, *Journal of ECerS*, 2021

# Phase-Field-Micromechanics Modeling of Microstructure Evolution in Solid-State Sintering

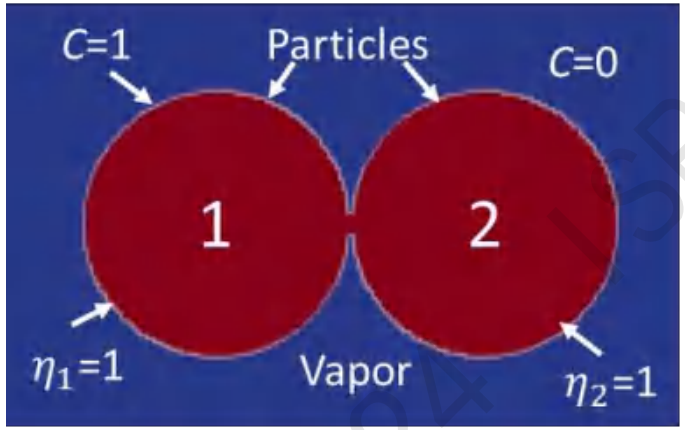


$$\mathcal{F} = \int_{\Omega} f\left(C, \eta_1, \eta_1, \ldots, \eta_{n_g}, \nabla C, \nabla\eta_1, \nabla\eta_2, \ldots, \nabla\eta_{n_g}\right) d\Omega$$

$$\frac{d\mathcal{F}}{dt} = -\left(\mathcal{D}_C + \sum_i^{n_g} \mathcal{D}_{\eta_i} + \mathcal{D}_m\right)$$

$$\mathcal{D}_C = \int_{\Omega} C^2 M^{-1} \left\|\dot{\mathbf{u}}_{\boldsymbol{g}}^{*}\right\|^2 d\Omega$$

Dissipation due to diffusions

$$\mathcal{D}_{\eta_i} = \int_{\Omega} L^{-1} \left\|\frac{\mathrm{D}\eta_i}{\mathrm{D}t}\right\|^2 d\Omega$$

Dissipation due of grain-grain interaction

$$\mathcal{D}_m = \int_{\Omega} \frac{1}{2}\mu^{eff} \left\|\nabla\dot{\mathbf{u}} + (\nabla\dot{\mathbf{u}})^{\mathrm{T}}\right\|^2 d\Omega$$

Dissipation due to grain motion

# Phase-Field-Micromechanics Modeling of Microstructure Evolution in Solid-State Sintering

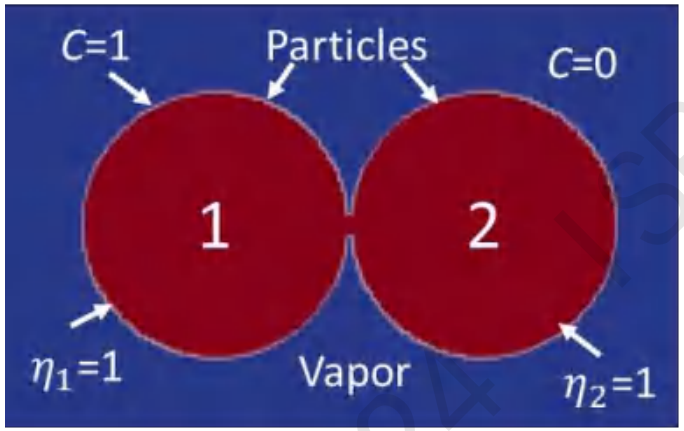


$$\mathcal{F}^* = \mathcal{F}^*_{sf} + \mathcal{F}^*_{gb}$$

$$N(C) = C^2[1 + 2(1 - C) + \epsilon(1 - C)^2],\ \epsilon > 3$$

$$\mathcal{F}^*_{sf} = \int_\Omega \left(\alpha C^2(1-C)^2 + \frac{\kappa_C}{2} \| \nabla C \|^2\right) \mathrm{d}\Omega$$

$$\mathcal{F}^*_{gb} = \int_\Omega N(C) \left(\beta \left[1 - 4\sum_{i=1}^{N_p} \eta_i^3 + 3\left(\sum_{i=1}^{N_p} \eta_i^2\right)^2\right] + \frac{\kappa_\eta}{2} \sum_{i=1}^{N_p} \| \nabla \eta_i \|^2\right) \mathrm{d}\Omega$$

## Governing equations:

$$\frac{\partial C}{\partial t} + \nabla \cdot (C\dot{\mathbf{u}}) = \nabla \cdot \left[M \nabla \frac{\delta \mathcal{F}}{\delta C}\right]$$

$$\nabla \cdot \boldsymbol{\sigma} + \mathbf{b} = 0$$

$$\boldsymbol{\sigma} = \mu^{eff}(\nabla \dot{\mathbf{u}} + (\nabla \dot{\mathbf{u}})^{\mathrm{T}}) + p\mathbf{I}$$

$$\frac{\partial \eta_i}{\partial t} + \dot{\mathbf{u}} \cdot \nabla \eta_i = -L \frac{\delta \mathcal{F}}{\delta \eta_i},\ i = 1,2,..,N_p,\ \boldsymbol{x} \in \Omega$$

$$\nabla \cdot \dot{\mathbf{u}} = 0$$

$\mathbf{b}$: surface tension and grain boundary tension

# Model Validation: Normal Stress along Grain Boundary

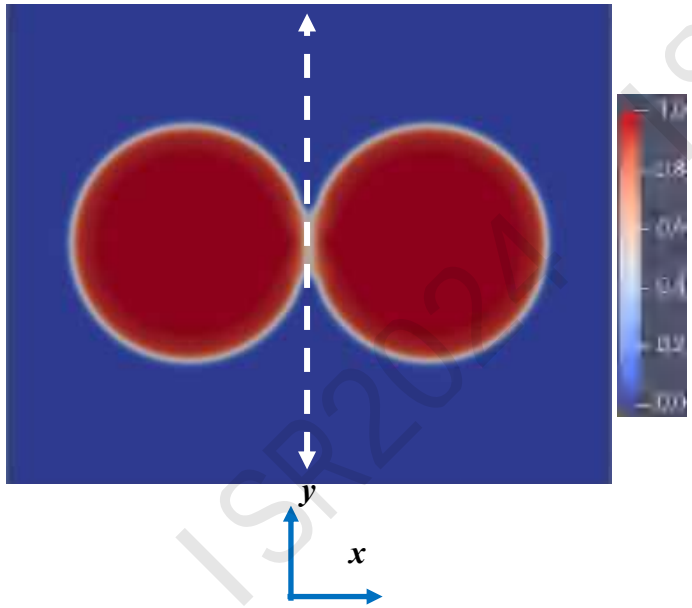


(a)

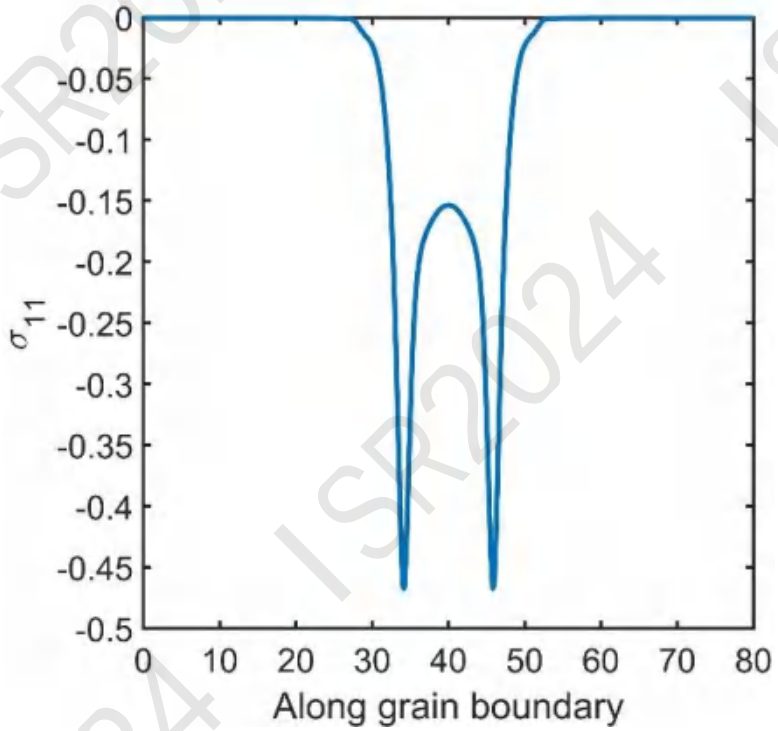


(b)

Normal stress distriubtion:

where $\kappa_{neck}$ is the curvature at the neck. The resulting normal stress distribution in the grain boundary is parabolic [5]:

$$\sigma_n = \gamma_s \kappa_{neck} + \frac{kT}{4\Omega\delta D_{gb}} \dot{u}_n (x^2 - r^2) \quad (7)$$

(a)The morphology of the two-particle model represented by $(C\eta_1)^2 + (C\eta_2)^2$ at 1200 timesteps and (b) the corresponding dimensionless normal stress ($\sigma_{11}$) distribution along grain boundary.

# Phase-Field-Micromechanics Modeling of Microstructure Evolution in Solid-State Sintering

## Stress distribution across the compact

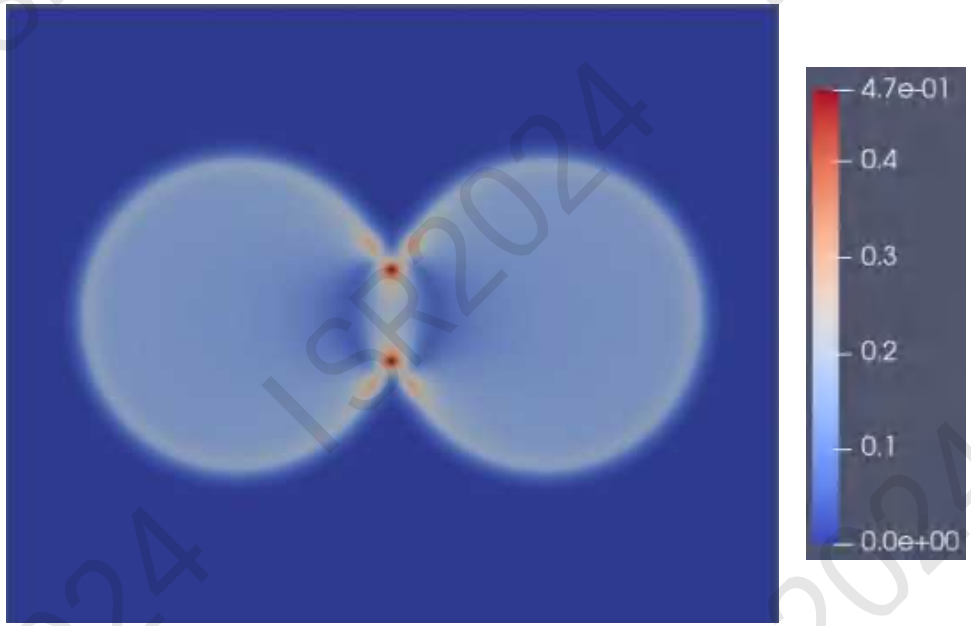


The distribution of $L_2$ norm of the dimensionless stress tensor across the two-particle compact at 1200 timesteps

# Model Validation: Sintering Neck Evolution

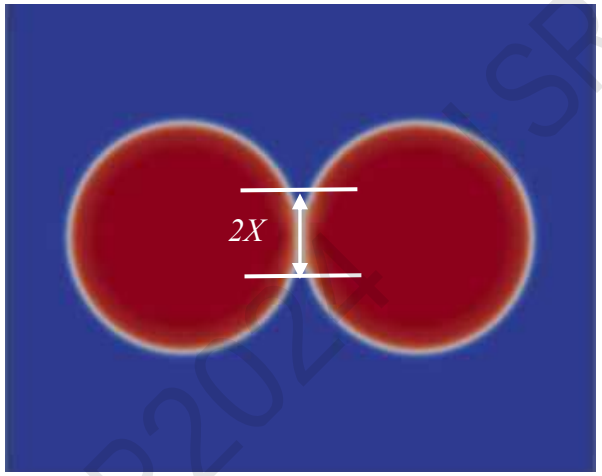


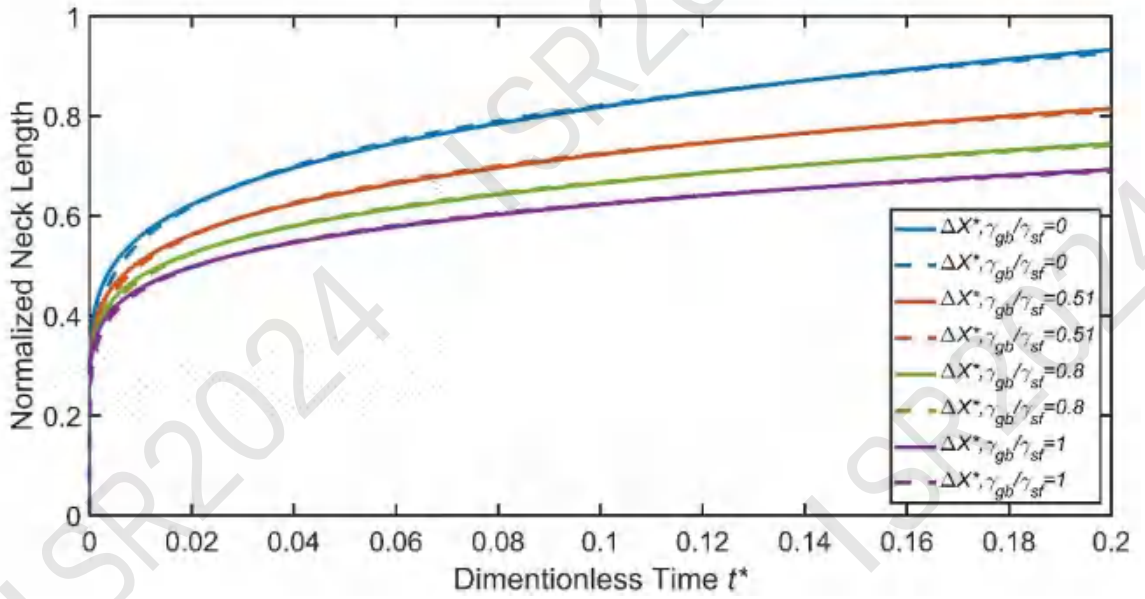


$$\frac{X}{r_0} = Bt^n$$

Theoretical value of $n$ base on rigid-body assumption is around 0.16

| $\frac{\gamma^{gb}}{\gamma^{sf}}$ | $n$ | $R^2$ |
|---|---|---|
| **0** | 0.1749 | 0.9983 |
| **0.51** | 0.1602 | 0.9986 |
| **0.80** | 0.1504 | 0.9988 |
| **1.0** | 0.1427 | 0.9989 |

# Model Validation: Shrinkage Strain

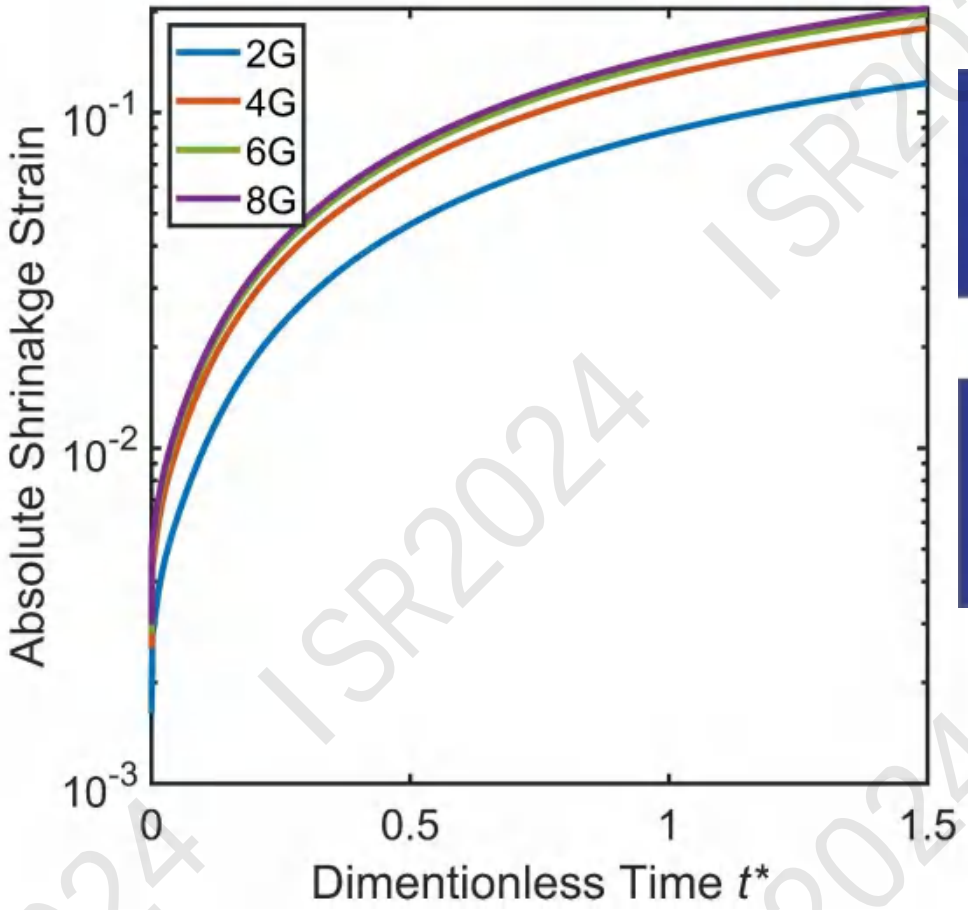


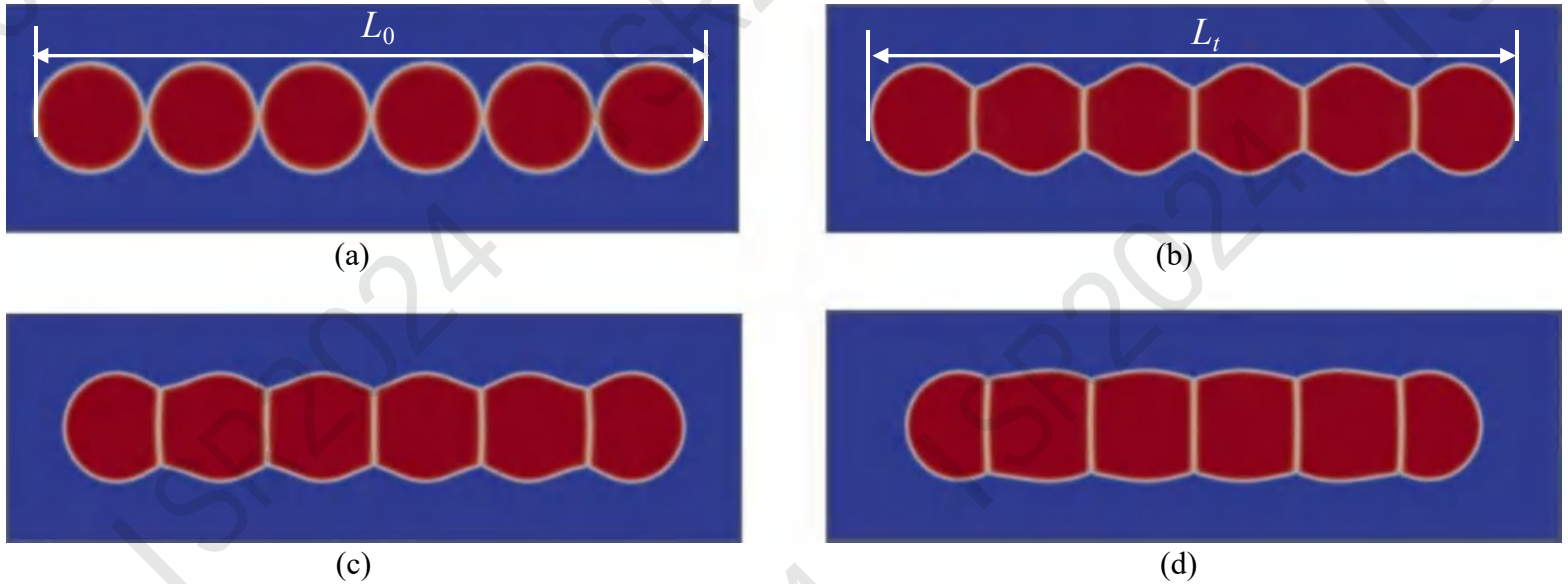


The microstructure morphology of the 6-grain chain at (a) initial, (b)1000, (c) 2000 and (d) 4000 timesteps. $L_0$ and $L_t$ represent the respective initial and current distances between the two ends of the particle chain.

$$\varepsilon_x(t) = \frac{L(t_0) - L(t)}{L(t_0)}$$

The densification strain $\varepsilon_x$ as a function of the normalize time $t^*$ for the respective 2-grain (2G), 4-grain(4G), 6-grain(6G) and 8-grain chains(8G).

# Experimental Validation: Sintering of $CeO_2$

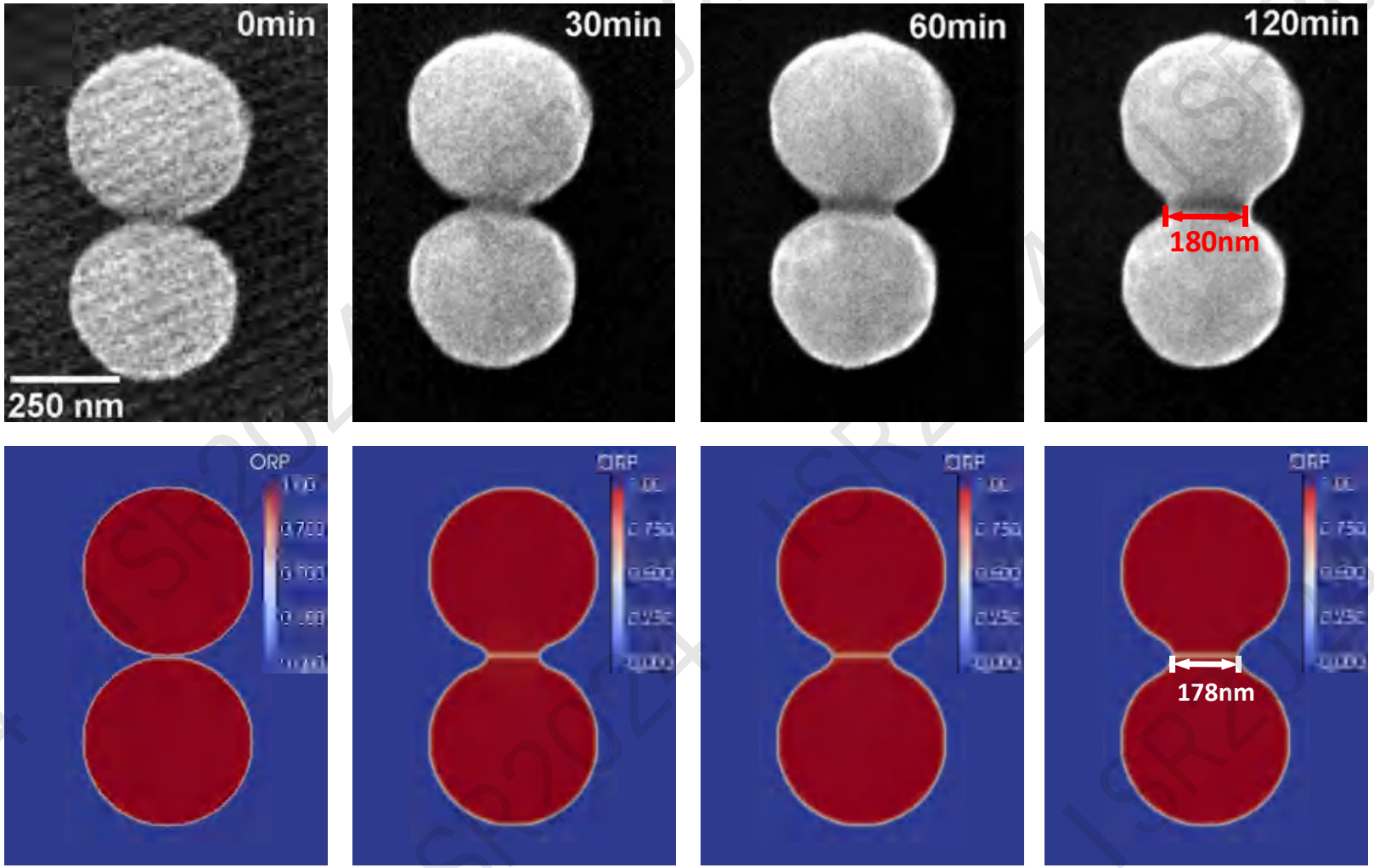


(a) t = 0min. (b) t = 30mins. (c) t = 60mins. (d) t = 120mins.

At 1050 Celsius degrees, CeO2 single crystal particles were sintered for 120 minutes, resulting in a neck length around 180 nm.

Our simulation results showed a neck length of 178 nm 。

# Applications： Effect of Particle Shape and Polycrystalinity

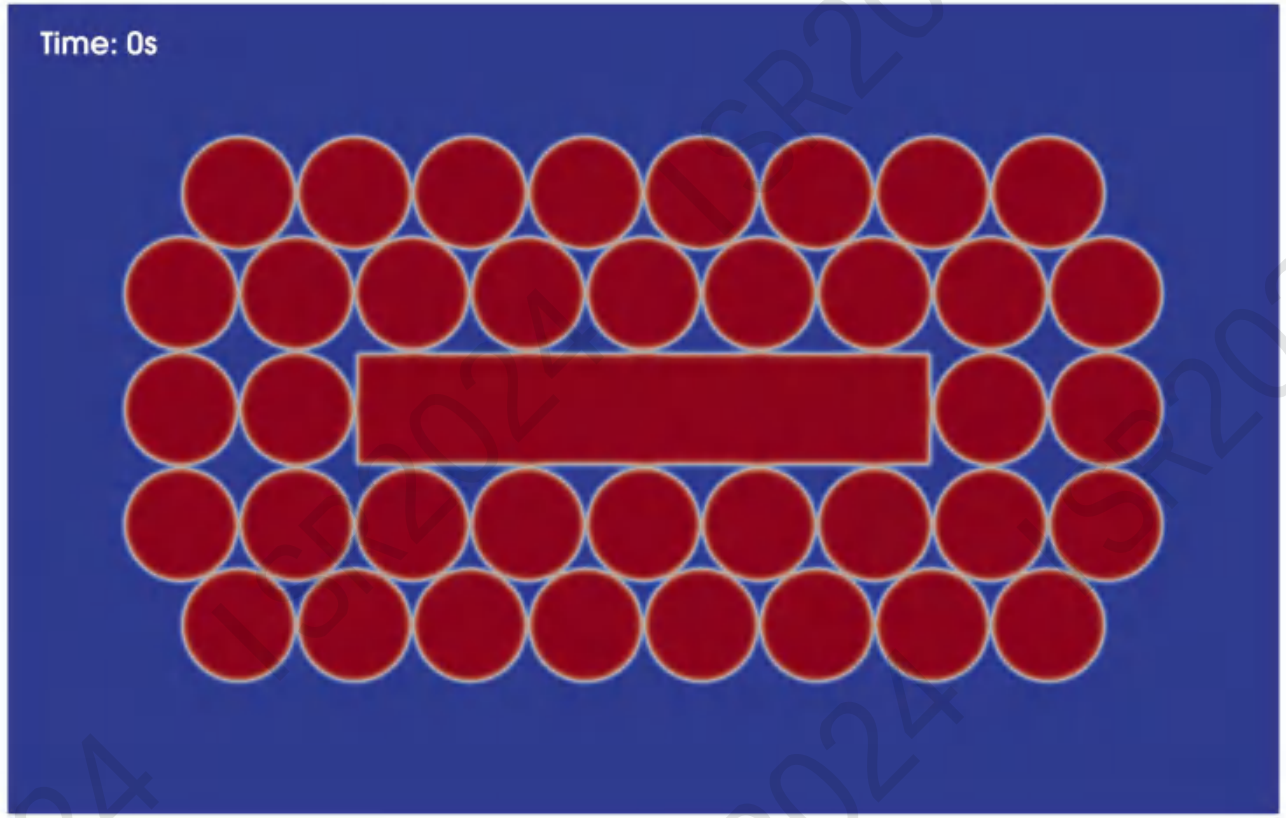


Effect of Particle Shapes

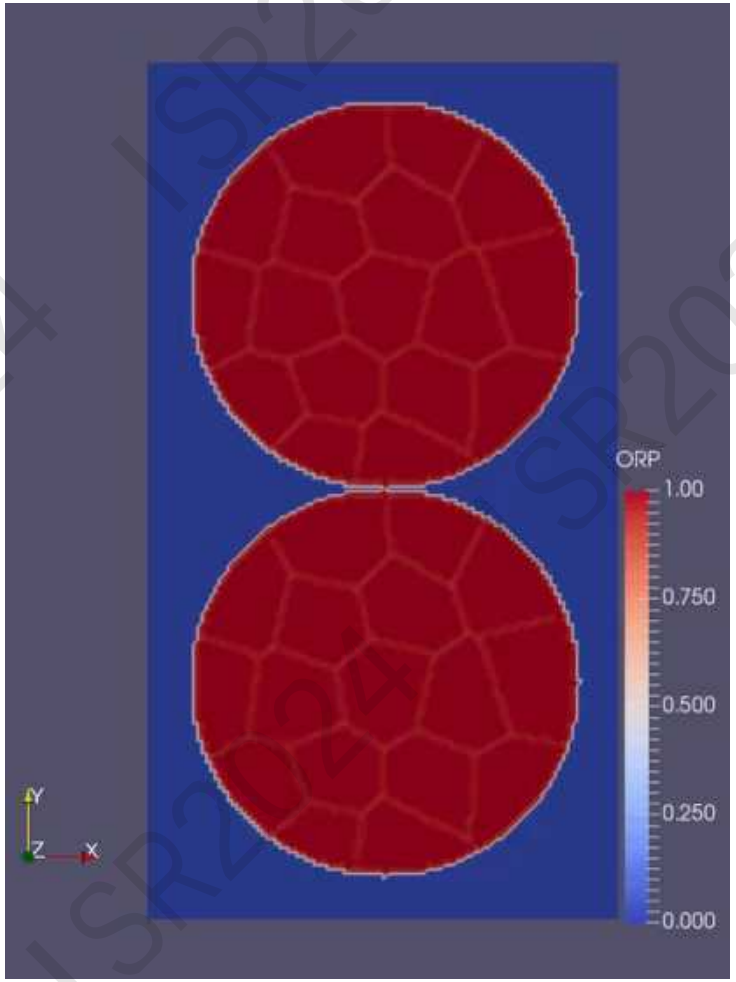


Effect of Polycrystallinity

# Application: Polycrystalline Effect

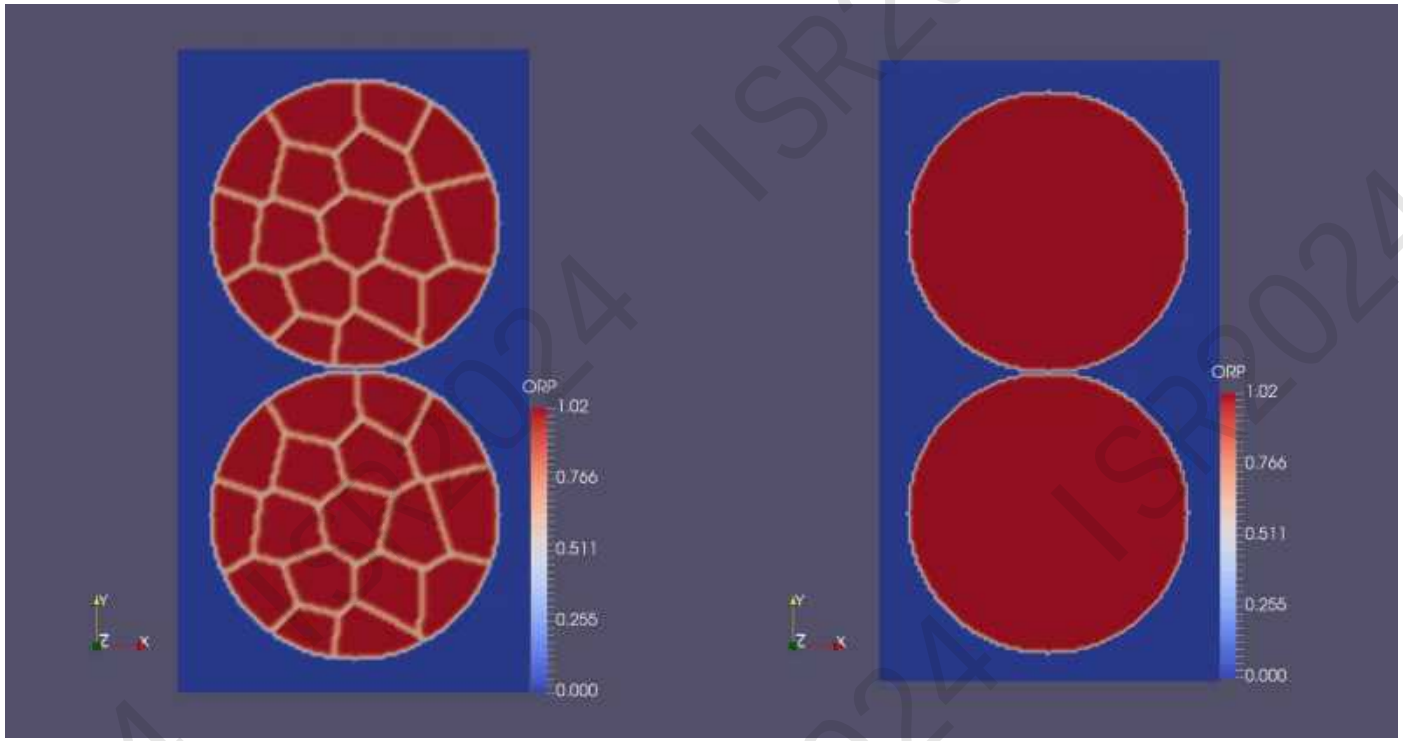


Polycrystalline Particles

Single-Crystal Particles

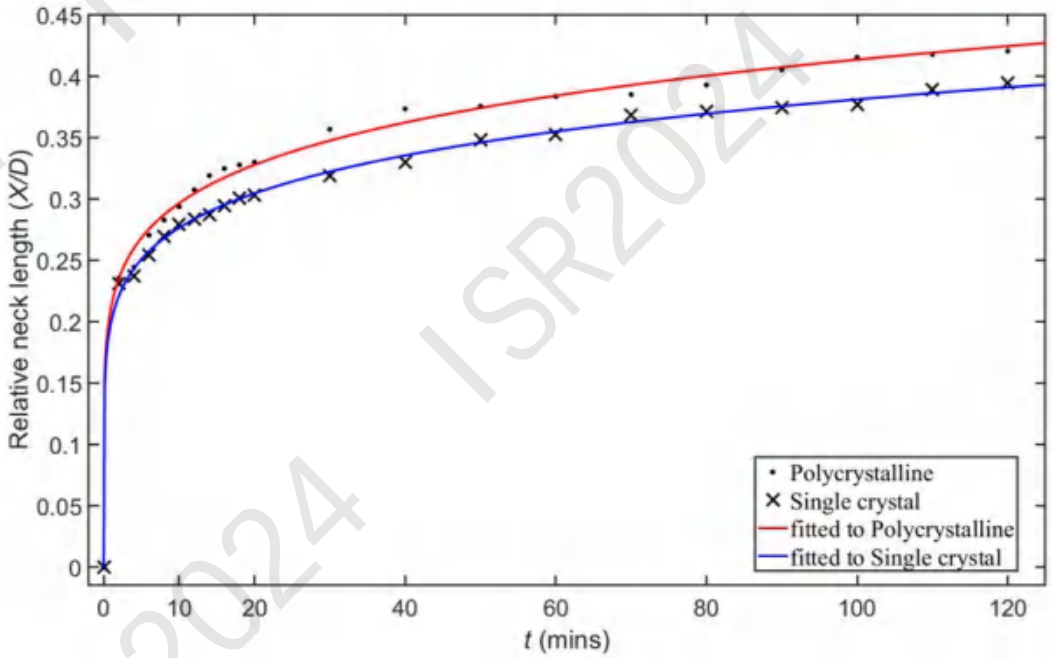


Normalized Neck Growth as a function of time

# Applications: Effect of Particle Size

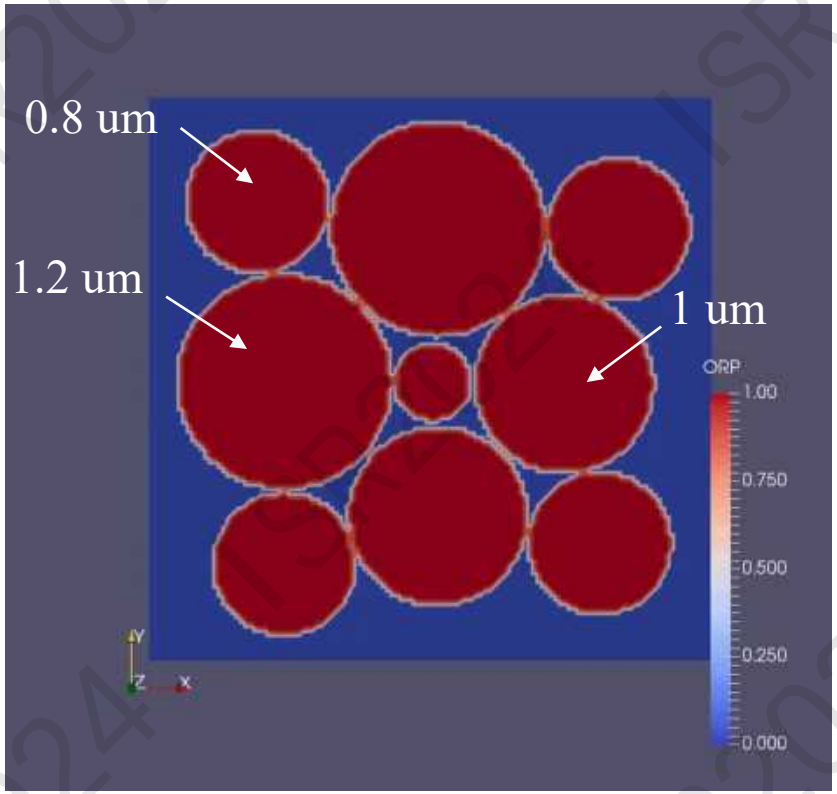


Microstructure Evolution of SiC under Sintering

# Summary

- Phase-Field-Micromechanics Modeling of Microstructure Evolution in Viscous Sintering: Polymers

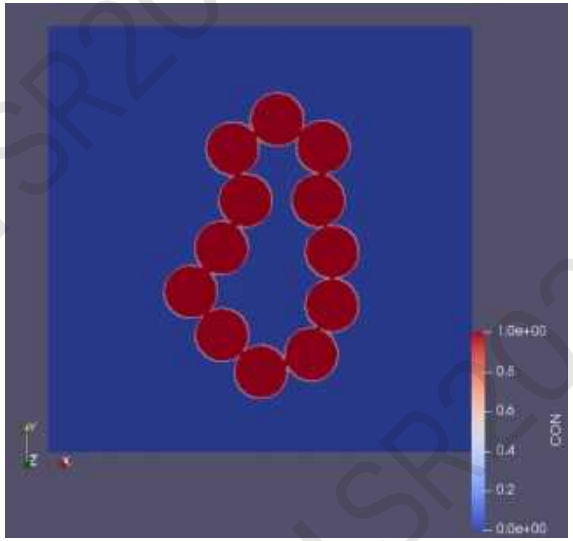


- Phase-Field-Micromechanics Modeling of Microstructure Evolution in Solid-State Sintering : Ceramics and Metals

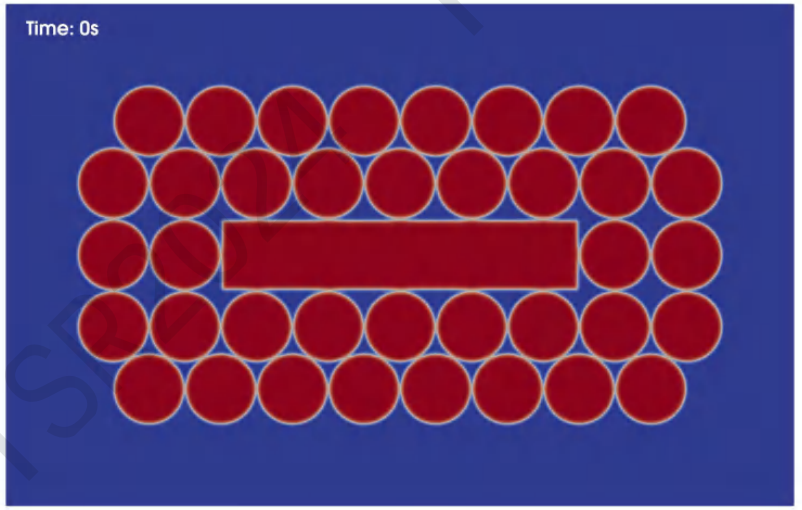

# Future work

- Multi-phase sintering involving both viscous sintering and solid-state sintering
- Pressure-assisted Sintering
- Field-assisted sintering
- Multiscale Modeling of Sintering and Sintering-based Additive Manufacturing

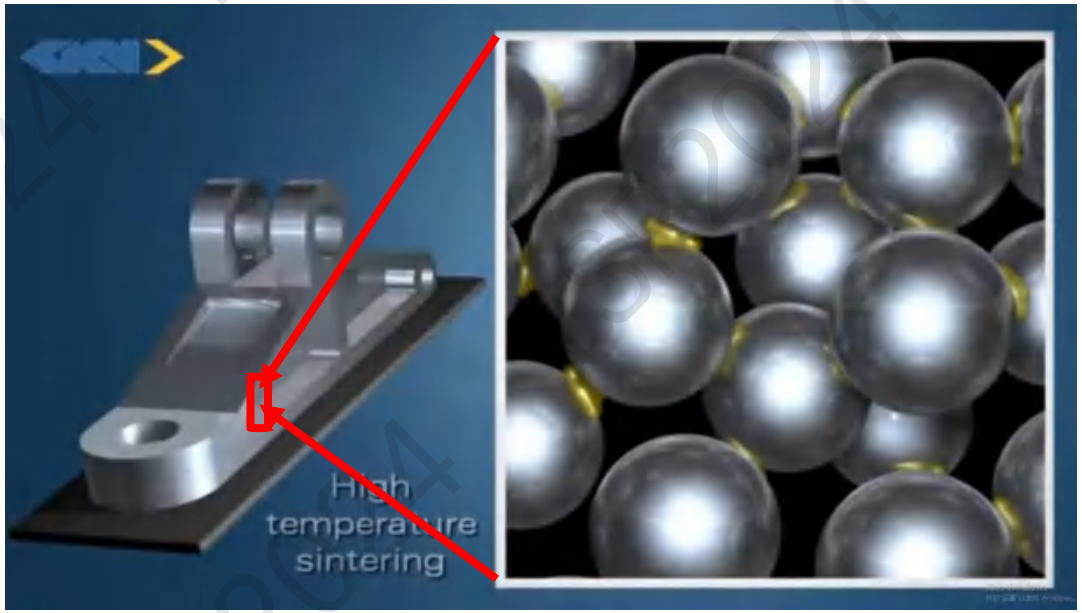

# Thank you!

qyang@shu.edu.cn

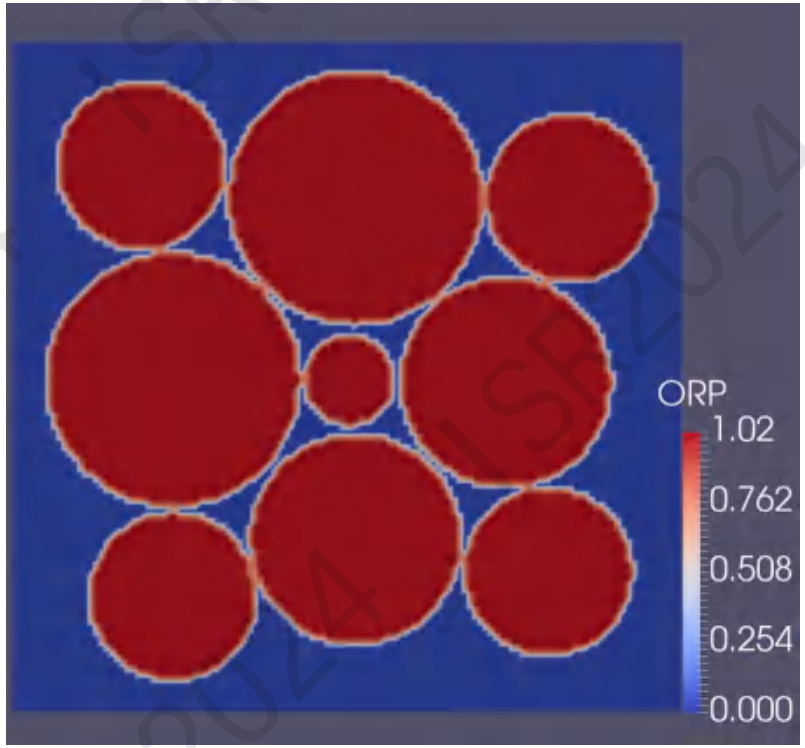

# Model Validation: Dihedral Angle

$\theta$: dihedral angle

The theoretical dihedral angle between two equal-sized particles at sintering equilibrium is given as:

$$\gamma^{gb} = 2\gamma^{sf}\cos\left(\frac{\theta}{2}\right)$$

$\gamma^{gb}/\gamma^{sf} = 1.5 \rightarrow \theta = 83^{\circ}$

$\gamma^{gb}/\gamma^{sf} = 1.0 \rightarrow \theta = 120^{\circ}$

$\gamma^{gb}/\gamma^{sf} = 1.5$

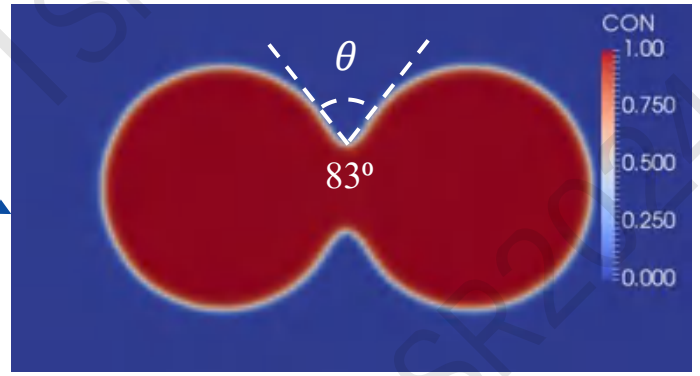


(a)

$\gamma^{gb}/\gamma^{sf} = 1.0$

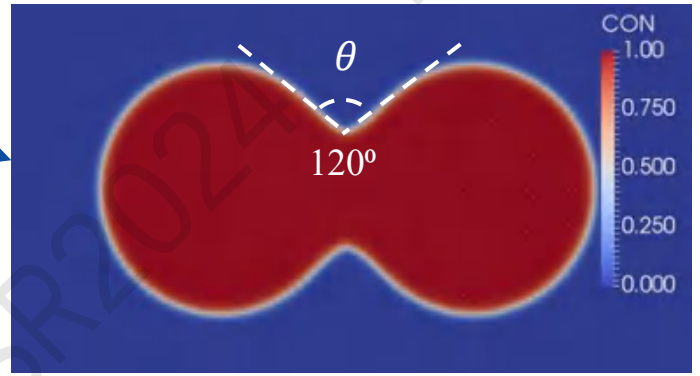


(b)

# Model Validation: Morphology

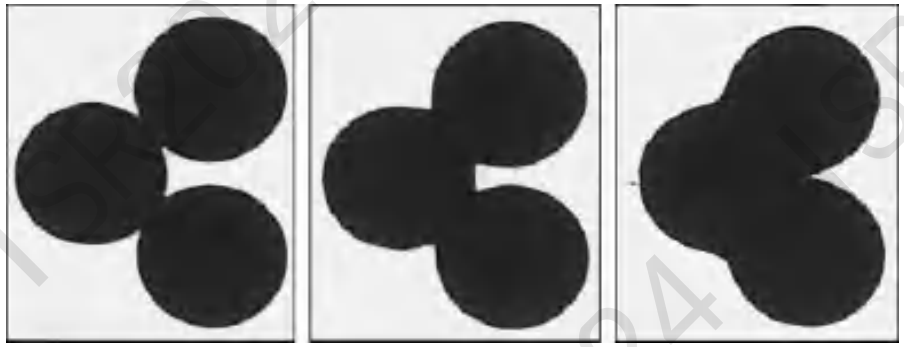

(a) Experimental observations

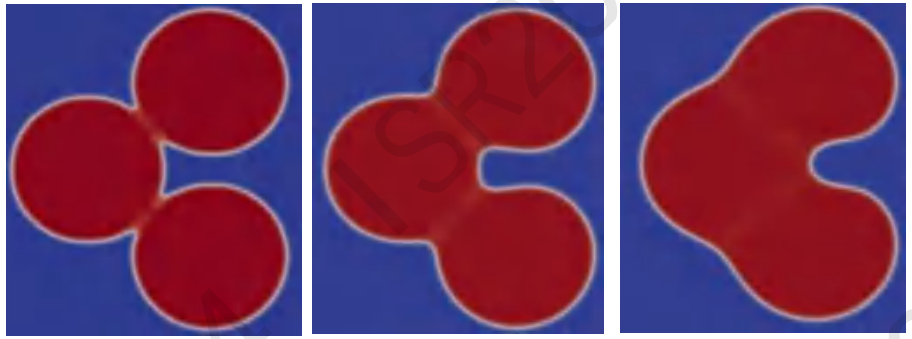

(b) Phase-Field simulation

Microstructure morphologies of a three-particle compact from experimental observations (a) (reproduced with permission from John Wiley and Sons) and phase-field predictions (b).

# Applications: Effect of Particle Size

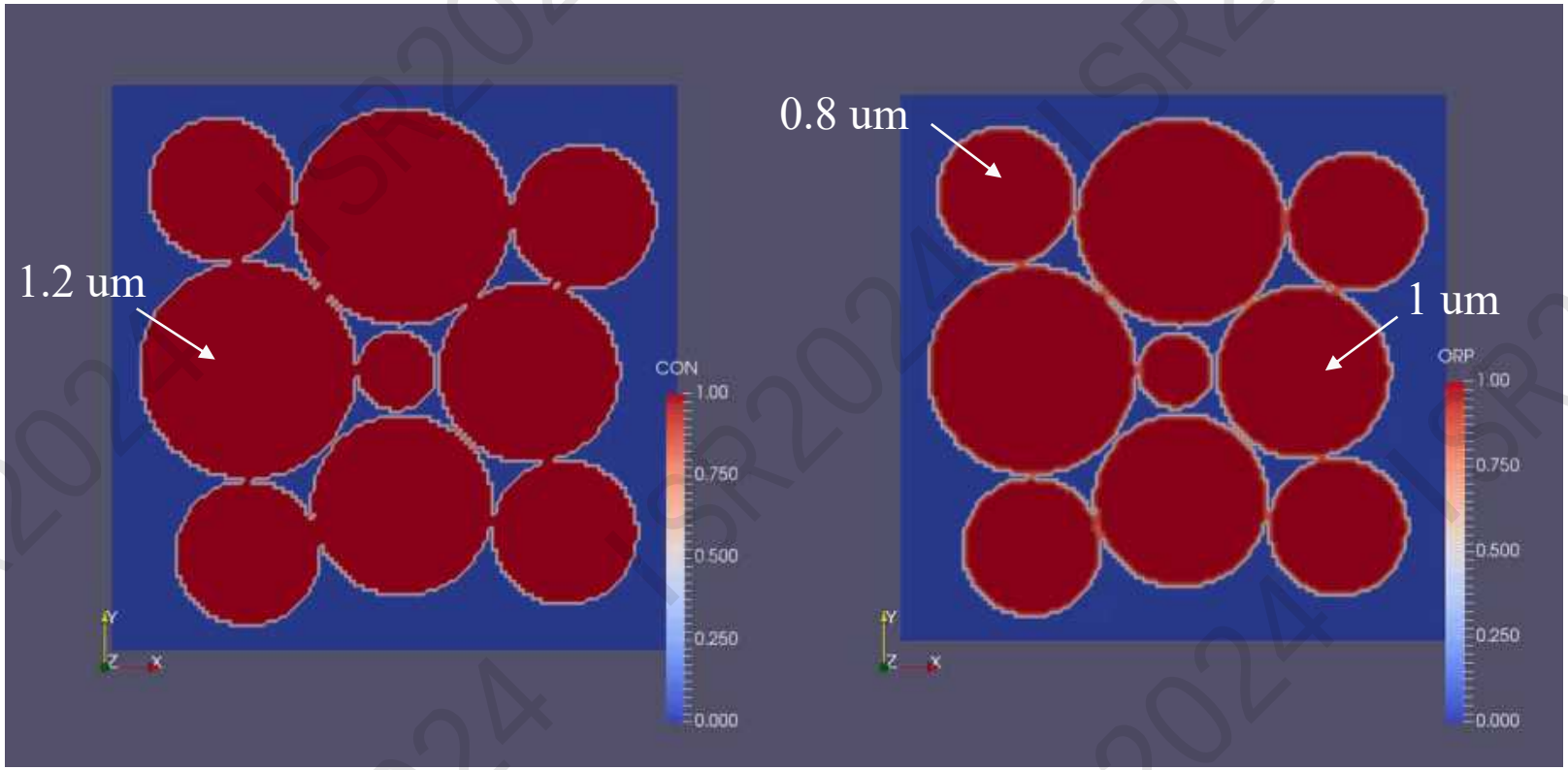


Microstructure Evolution of SiC under Sintering